Synthesizing and processing conducting polythiophene derivatives for charge dissipation in electron-beam lithography

Wu-Song Huang
IBM Microelectronics Division, Hopewell Junction, New York 12533, USA
(Received 27 December 1993; revised 15 March 1994)

In electron-beam lithography, charging on the photoresist usually causes image distortion and placement error. To dissipate the charge, a conductive polymeric layer can be introduced either over or under the photoresist coating. In this paper, we will discuss the approach of using toluene and xylene-soluble poly(alkylthiophene) in combination with a photoacid generator as a discharge underlayer or interlayer beneath the photoresist to dissipate the accumulated charge during electron-beam exposure. We will also discuss the use of water-soluble acid or ammonium salt forms of poly[3-(ethanesulfonate)thiophene] as the discharge top layer. During the resist image developing process, the top layer will be removed by aqueous base. Therefore, it is advantageous to use a discharge top layer owing to its simplicity. In this study, the salt and acid forms of poly[3-(ethanesulfonate)thiophene] were synthesized through chemical polymerization of the corresponding methanesulfonate ester. They exhibit the same properties as those of electrochemically synthesized polymer reported in the literature.

(Keywords: polythiophene derivatives; synthesis; conducting polymers)

INTRODUCTION

In electron-beam lithography, many studies have shown that resist charging during electron-beam exposure can lead to image distortion and pattern placement error[1–4]. Recently, a few approaches have been proposed to solve this charging problem using organic materials as discharge layers. These organic materials, usually polymeric, can be spin-coated either on top or under the resist to form a conductive layer for charge dissipation. These polymeric materials have to be conductive; they include ionic conductive materials such as ammonium poly(*p*-styrene sulfonate)[5,6] and surfactants[7], etc., and electrically conductive materials such as the charge-transfer complex–polymer salt of poly(vinylbenzyl triethylammonium)–TCNQ[8] (tetracyanoquinodimethane) and protonic acid-doped polymer of polyaniline[9,10]. I have investigated the use of ammonium poly(*p*-styrene sulfonate) as the discharge top layer in our system. I found this polymer not conductive enough to eliminate completely the charging effect on the resist. However, a significant reduction in charging on the resist was found. It is obvious that the higher the conductivity of the polymer, the less charging effect will occur on the resist. Based on this principle, I have investigated the family of electrically conductive polythiophenes for this charge dissipation application, and report the experimental findings in this paper.

POLYMER SYNTHESIS AND DOPING

Since the discovery of polyacetylene as a conducting polymer 16 years ago[11], many new conducting polymeric materials have been developed. Among these polymers, polythiophene and its derivatives have gained considerable attention owing to their high conductivity and remarkable stability[12]. Polythiophene is not a processable polymer. However, it has been reported that incorporation of long, flexible alkyl side chains into the 3-position of the thiophene ring allows the polymer to become soluble in some organic solvents, e.g. xylene, toluene, etc.[13]. In addition, introduction of a side chain containing a sulfonate functional group allows the polymer to become water-soluble[14]. In this paper, we will report the use of poly(alkylthiophene) as a discharge interlayer under a photoresist, and the use of water-soluble polythiophene derivative as discharge top layer.

Polyalkylthiophenes

Most of the conducting polymers are obtained from their insulating forms by exposing these materials to toxic vapours such as ASF_5, SbF_5, I_2, etc., or immersing these materials in solutions containing a strong oxidizer like $NOPF_6$, $HClO_4$, etc. These are usually not acceptable to the manufacturing process. In my approach, I mixed poly(alkylthiophene)s with a photoacid generator and then subjected them to u.v. exposure to convert these polymers to conducting forms. The poly(alkylthiophene)s used in this study are poly(3-butylthiophene) and 3-methylthiophene copolymer (PMBT).

It has been reported that polyacetylene[15] and polypyrrole[16] can be photochemically doped by dipping films of the material into a solution of the triarylsulfonium and diaryliodonium salts and subsequently exposing the films

0032-3861/94/19/4057–08
© 1994 Butterworth-Heinemann Ltd

to ultraviolet (u.v.) radiation. In these systems, non-processable polymers were used. A processable polymer like polyaniline was reported to have uniformly blended in solution with the onium salt[17]. Since these onium salts are known to decompose upon u.v. radiation to generate protonic acids[18,19], this photochemical doping process is commonly rationalized as a protonic acid doping process. This explanation may be true for polyaniline, but it may not be true for other conducting polymers. A study by Saeva and Morgan[20] shows that the radical cation of aryl sulfide generated in the photodecomposition process of onium salt has oxidation potential >1.0 V (vs. SCE). This high oxidation potential is sufficient to oxidize polythiophenes (for PMBT, $E_{1/2} = 0.7$ V vs. SCE)[21,22], polyacetylene and polypyrrole. Therefore, it is very conclusive that the photodoping process is through oxidation rather than protonic acid.

Poly(alkylthiophene)s are more soluble in toluene and xylenes than in some polar solvents such as tetrahydrofuran, 1-methyl-2-pyrrolidinone (NMP) and anisole, etc. On the other hand, onium salts are soluble in NMP but insoluble in xylenes. Therefore, to obtain a homogeneous blend of poly(alkylthiophene)s and onium salt, I have to adopt a mixed solvent of NMP and xylene. Owing to this problem, I have switched to a new photoacid generator developed in IBM. This new compound is a sulfoxyimide-type non-ionic photoacid generator (SFPAG) that is soluble in xylenes. Good mixing has been achieved between poly(alkylthiophene)s and SFPAG in xylenes. We also found that spin-coated films were more homogeneous in this system than that in the onium salt system. The typical composition of this conducting polymer solution contains approximately 12% solid content in xylene with 11% SFPAG in PMBT. To examine the conductivity achievable by this system, the above solution was spin-coated onto an SiO_2/Si wafer and then subjected to u.v. exposure for 15 min. Afterwards the wafer was baked on a hot plate for 40 s at 90°C. A conductivity of 0.1 S cm^{-1} was measured on the polymer coating using the four-probe method. With the exposure tools that we used, 15 min exposure would output around 1 J cm^{-2}. One reason for the requirement for this high dose is the high absorption of PMBT in the deep u.v. range and the low quantum efficiency of SFPAG. Another reason is that this photodoping process needs a large portion of the photoacid generator decomposed, while regular chemical amplified resist system only needs a trace amount of acid generated in the resist for chemical amplification.

Water-soluble polythiophene derivatives

In the reported literature[14], acid and sodium salts of poly[3-(2-ethanesulfonate)thiophene] were synthesized through electrochemical polymerization of the methyl 2-(3-thienyl)ethanesulfonate, followed by conversion to the polyelectrolyte via sodium iodide in acetone. The synthetic procedure is shown in *Figure 1a*. Using the same approach, we found it difficult to collect a sufficient amount of material for the discharge test through this electrochemical method. Therefore, we polymerized methyl 2-(3-thienyl)ethanesulfonate in nitromethane with ferric trichloride, then converted this methyl ester polymer to the sodium salt of poly[3-(2-ethanesulfonate)thiophene] (P3-ETSNa) via sodium iodide in acetone. The acid form of the polymer can be obtained through the treatment of acidic ion-exchange resin. With this chemical polymerization, the yield of the polymer is above 90%, in contrast to the very

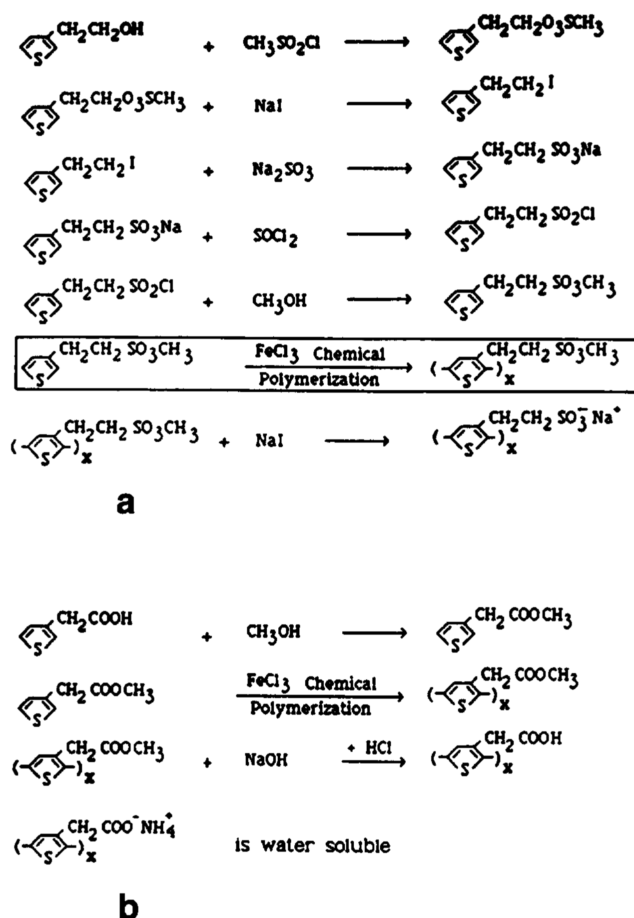

Figure 1 Synthetic schemes for (a) poly[3-(ethanesulfonate)thiophene] and (b) poly(3-thiophene acetate)

low yield obtained through electrochemical polymerization. The above chemical polymerization was carried out in non-aqueous medium. The synthesis of sodium salt of poly[3-(3-thienyl)propanesulfonate] by chemical polymerization with ferric trichloride in aqueous medium was reported by Ikenoue *et al.*[23].

The optical properties of chemically made material are similar to those of electrochemically made material as evidenced in the optical absorption spectrum shown in *Figure 2*. The absorption maximum in the spectrum here is at 425 nm, exactly the same as that reported in the literature of the electrochemically made polymer[24]. I also found that the acid and sodium salt forms gave the same type of spectrum. However, when the aqueous polymer solution was added in with a small amount of ammonium persulfate, the solution turned blue black and the spectra became very different as shown in *Figure 3*. These spectra are an indication of the existence of positive charges on the polymer backbone, commonly described as bipolarons. The change of the spectrum was fast in the first 18 h and slowed down when the amount of charge carriers on the backbone was decreased. The polymer solution can remain blue for five or six days. It does not remain self-doped like the acid form of poly[3-(propanesulfonate)thiophene] chemically synthesized in aqueous medium using ferric trichloride as an oxidizer by Ikenoue *et al.*[23]. However, if the blue black methyl ester polymer synthesized from ferric trichloride was treated with sodium iodide and then 1 M HCl for a few days, it seems to have the tendency to be self-doped. This may be due to the existence of residue

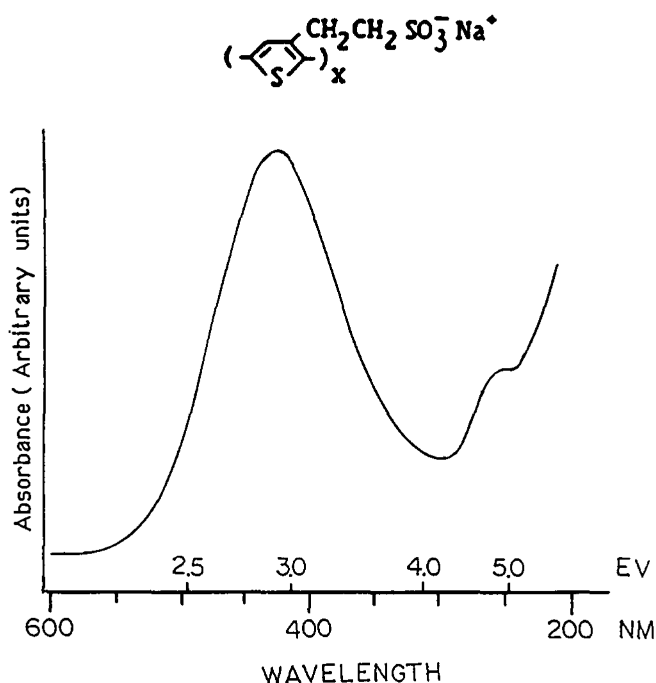

Figure 2 Absorption spectrum of chemically synthesized sodium salt of poly[3-(ethanesulfonate)thiophene]

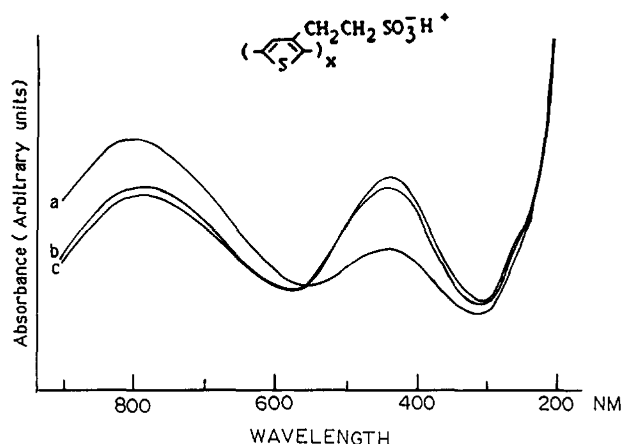

Figure 3 Absorption spectra of ammonium persulfate-treated acid form of poly[3-(ethanesulfonate)thiophene] in water for different sitting time: fresh (curve a), 18 h (curve b) and 24 h (curve c)

ferric ions, which continue to oxidize the polymer and allow the polymer molecular weight to continue to grow. The chemically made polymer is electroactive and has an electrochromic effect as shown in *Figure 4*. During the anodic scan, the colour of the polymer film changed from orange to blue black, then was reversed during the cathodic scan.

The success of using P3-ETS as a discharge top layer prompted us to search for other alternatives that would be easier to synthesize. One approach was to move from the sulfonic acid derivative to the carboxylic acid derivative of polythiophene. Therefore, 3-thiopheneacetic acid was reacted with methanol to form its methyl carboxylic ester. Polymerization was carried out in the same way as making methyl ester of P3-ETS. The conversion of acetate ester polymer to acetic acid polymer was accomplished by refluxing it in sodium hydroxide aqueous solution, then precipitating out in HCl. The synthetic procedure is shown in *Figure 1b*. The obtained ammonium poly(3-thiophene acetate) is not electroactive as shown in *Figure 5*, and is not conductive. On the contrary, the methyl ester of this polymer is electroactive as shown in *Figure 6*, just like the methyl ester of P3-ETS. *Figure 7* shows a different ester polymer synthesized from 2-(3-thienyl)ethyl methanesulfonate (the compound synthesized at the first step in *Figure 1a*). All these ester polymers are soluble in some organic solvents. Despite the fact that they cannot be used as top layer, they can be used as discharge underlayer like poly(alkylthiophene)s.

METHOD FOR DISCHARGE TEST

To examine the charging effect on resist during electron-beam exposure, the 'Hontas discharge test' is usually performed before pursuing any test on the manufacture production line. It appears to be a reliable functional test. The test uses a Hontas tool (IBM E-beam system) at 25 keV with a dose of 15 μC cm^{-2}. Two chips are written on one wafer. Each chip has the pattern shown in *Figure 8*.

Charge inner: The electron beam moves from right to left, then from left to right in a continuous fashion. The beam writes the 400 small squares (2 μm × 2 μm) first. Each square is located at 250 μm apart in both directions. This

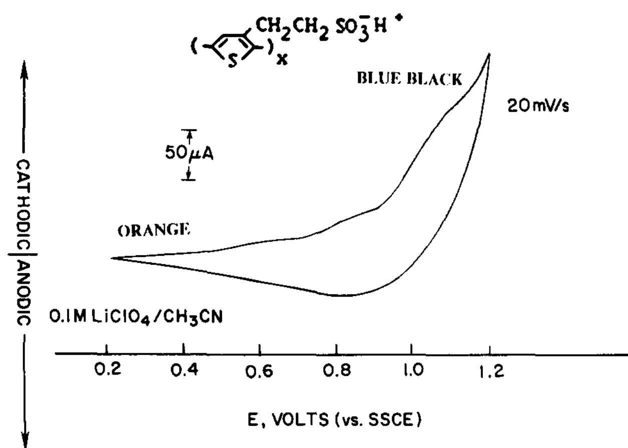

Figure 4 Cyclic voltammogram of acid form of poly[3-(ethanesulfonate)thiophene] on Pt in 0.1 M $LiClO_4/CH_3CN$ at 20 mV s^{-1} scan rate between 0.2 and 1.2 V (vs. SSCE)

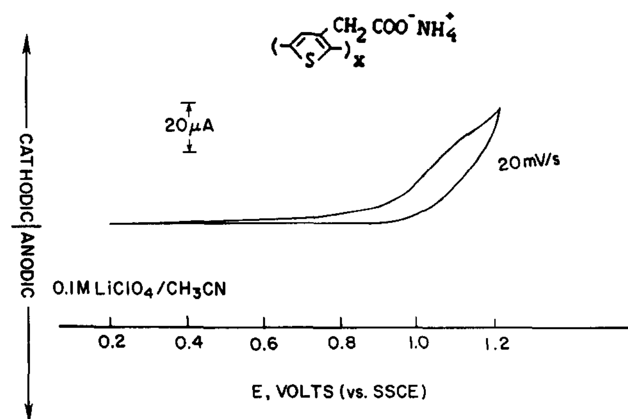

Figure 5 Cyclic voltammogram of ammonium poly(3-thiophene acetate) on Pt in 0.1 M $LiClO_4/CH_3CN$ at 20 mV s^{-1} scan rate between 0.2 and 1.2 V (vs. SSCE)

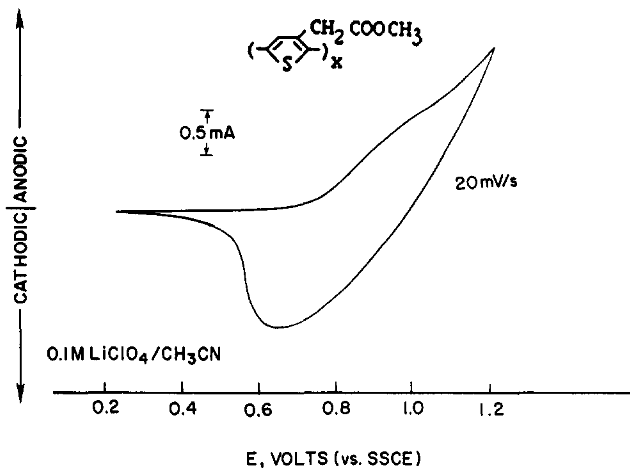

Figure 6 Cyclic voltammogram of poly(3-thiophene methyl acetate) on Pt in 0.1 M $LiClO_4/CH_3CN$ at $20\,mV\,s^{-1}$ scan rate between 0.2 and 1.2 V (vs. SSCE)

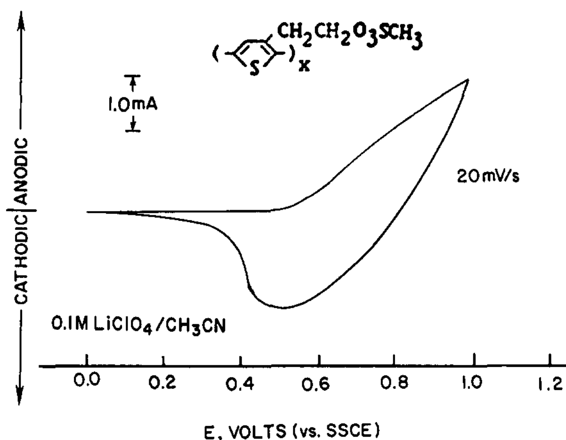

Figure 7 Cyclic voltammogram of poly[2-(3-thienyl)ethyl methanesulfonate] on Pt in 0.1 M $LiClO_4/CH_3CN$ at $20\,mV\,s^{-1}$ scan rate between 0.0 and 1.0 V (vs. SSCE)

will give a density of 6.2×10^{-3} per cent. Since the density is low, no charging will occur on these squares.

Charge outer: The electron beam is then moved to the top-right corner and starts to expose the whole chip area except the 10 μm squares around the small 2 μm squares. This pattern has a density of 99.86%.

In this test, the inner square is acting as a reference. When there is no charging effect, the 2 μm square will always reside at the centre of the 10 μm square (see *Figure 9*). If there is charging on the resist, the 2 μm square will move away from the centre. In general, the first one at the top-right corner has very little effect by charging owing to the small exposed area. On the other hand, the last one (400th) at the bottom-left corner will have a strong influence by the charging owing to the high density of the exposed area. The displacement of the 2 μm square away from the 10 μm square centre will give a qualitative indication of the extent of charging on the resist. The charging phenomenon is simply due to the electrons trapped on the resist and starts to build up a potential on the surface. This negative electrical field then repulses the incoming electron beam away from the set target point and consequently distorts the image pattern on the resist.

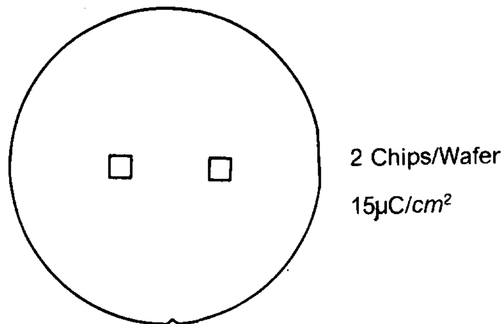

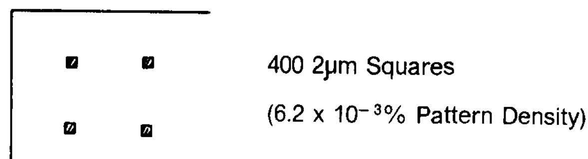

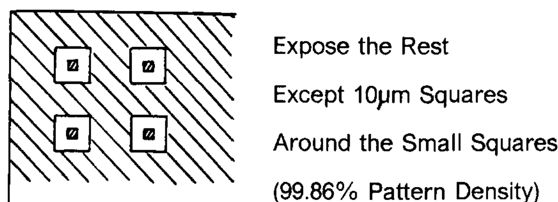

Figure 8 An illustration of the electron-beam charging test pattern. The exposures are performed with a 25 keV system

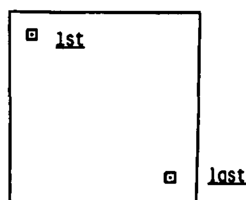

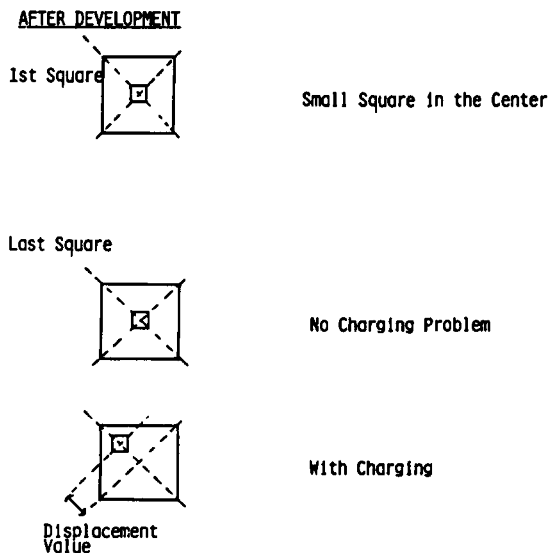

Figure 9 An illustration of the measurement of displacement value (electron-beam landing error) caused by charging on the resist

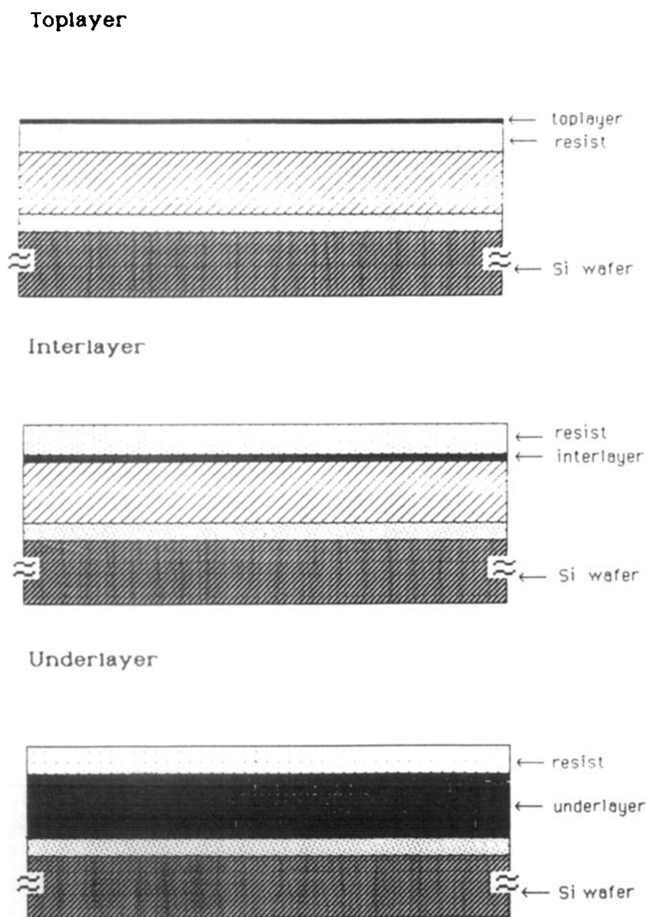

Figure 10 The three possible ways that conductive discharge layer can be incorporated into a multilayer resist system

DISCHARGE TEST USING CONDUCTING POLYMERIC DISCHARGE LAYER

There are three ways to put a discharge layer into multilayer resist systems. As shown in *Figure 10*, it can be introduced as top layer, interlayer and underlayer respectively. When a water-soluble conductive polymeric top layer is introduced, it is removed during the resist image developing process in an aqueous developable resist system. Both underlayer and interlayer need an oxygen plasma etching process to etch through it. All these three systems are workable in the manufacturing process. However, it is advantageous to use a discharge top layer owing to its simplicity.

Discharge test using conductive interlayer

A Si wafer containing 5000 Å of SiO_2 on the surface was spin-coated with AZ 4210 and then subjected to 230°C oven bake for 30 min. The thickness of the hard baked AZ resist (HBAZ) obtained from this process was approximately 2.7 μm. The total thickness of the whole insulating stack on the surface of Si was then increased to 3.2 μm. TNS resist was then coated on top of the above assembly, then subjected to the Hontas discharge test. The result is shown in *Figure 11*. A large electron-beam landing offset was found on the last (400th) square, due to a charging effect on the resist. It is obvious that the system needs a discharge layer to disspate the charge accumulated on the resist surface. The polymeric discharge layer experiment was carried out by spin-coating a layer of poly(alkylthiophene)s + SFPAG (0.4 μm) on top of HBAZ as a conductive discharge interlayer, then subjected to 45 min u.v. exposure followed by 86°C hot-plate bake. TNS was then coated on top of this assembly for discharge test. The result is shown in *Figure 12*. No charging effect was found on the resist. The 2 μm square remains at the centre of the 10 μm square on the last spot (400th). This experimental result clearly indicates that the charging effect has been eliminated by introducing this conductive interlayer.

Discharge test using conductive top layer

As mentioned earlier, the uncleaned P3-ETS treated with HCl for a few days had higher tendency to be self-doped. This polymer was precipitated out from aqueous HCl solution by adding it to a copious amount of acetone. It was then redissolved in water and treated with ion-exchange resin. The polymer ammonium salt solution was obtained by neutralizing the polymer acid with ammonium hydroxide. When a layer of the above-described ammonium polymer salt around 600 Å was coated on top of TNS resist, less charging was observed

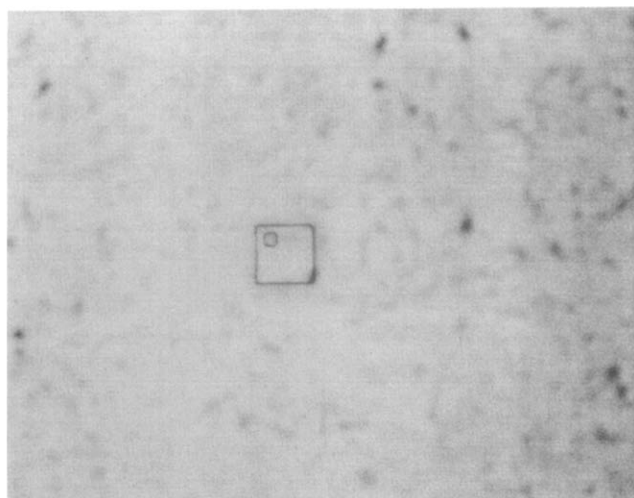

Figure 11 Charging test result for the last square (400th) of a control wafer (without discharge layer)

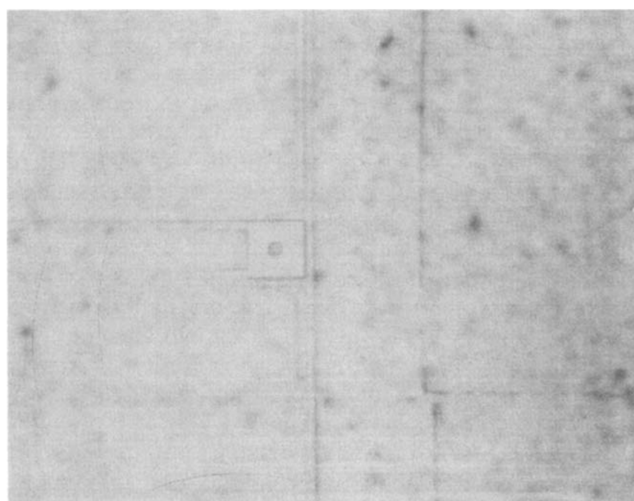

Figure 12 Charging test result for the last square (400th) of a wafer using PMBT + SFPAG blend as discharge interlayer

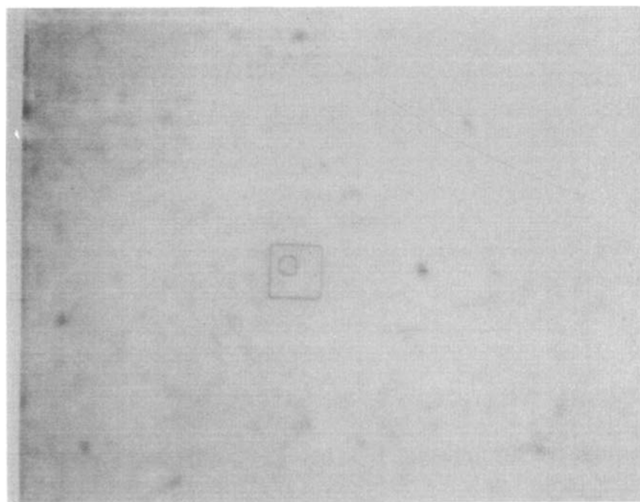

Figure 13 Charging test result for the last square (400th) of a wafer using ammonium poly[3-(ethanesulfonate)thiophene] as discharge top layer

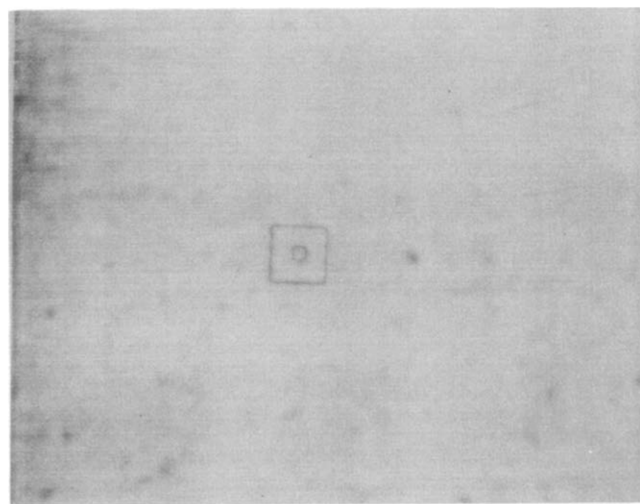

Figure 14 Charging test result for the last square (400th) of a wafer using ammonium poly[3-(ethanesulfonate)thiophene] plus trace amount of sulfuric acid as discharge top layer

in comparison to that of control. This is shown in *Figure 13*. While I added a trace amount of sulfuric acid to convert the polymer back to partial acid form and applied this polymer on top of TNS resist as discharge layer with thickness around 1000 Å, no charging was observed on the resist image at all (see *Figure 14*). I believe the slightly acidic environment may stabilize the polycarbonium ion in the backbone, which leads to higher conductivity on the polymer. Since P3-ETS synthesized here usually does not have self-doped behaviour, I found that the system was more reliable by adding a trace amount of ammonium persulfate to the polymer solution before it was applied on top of the resist. The composition of this conducting polymer solution included 700 mg of P3-ETSH, 16 ml of water and 20 mg of ammonium persulfate. With spin speed in the range of 2000–2500 rev min^{-1}, the spin-coated conductive top layer is around 900–1200 Å. No charging on the resist was found in the Hontas discharge test when this discharge top layer was used.

DISCUSSION AND CONCLUSION

It has been verified that the increase of charging is faster than the increase of the resist thickness. A conducting interlayer only affects the charging of the layers underneath. The resist layer on top of it still charges up. If the resist is not too thick, we can assume that all the charge accumulated on the resist will immediately leak to the conductive interlayer and flow to ground. The charge has to leak away quickly enough not to build up any significant potential at the target point. The discharge mechanism for the top layer is basically the same as for the interlayer except that there is no insulator on top of it. Based on the formation of a capacitance between this conductive layer and the Si substrate, the time needed to discharge a capacitor through a *RC* circuit has to be shorter than the exposure cycle time. I will discuss this later. We just approach the problem in a simple way by assuming that there is a simple resistor between target point and ground. We also assume that electron-beam current is flowing between target point and ground through this resistor. Because the Hontas tool has a beam current of 4 μA, the simple equation $IR=V$ will give you the value of approximately 10^{-6} S required for this circuit to keep the voltage difference between target point and ground within single digits. For a 1 μm film to achieve this kind of surface conductivity, it only needs a volume conductivity of 10^{-2} S cm^{-1}. A 1000 Å film needs a conductivity of 10^{-1} S cm^{-1}. Since electrons penetrate through resist, conductive interlayer and insulator stack underneath, at the same time producing secondary electrons and back-scattering electrons, the system is not as simple as what we describe above. Other factors like electron-beam-induced conductivity and local heating effect make the problem even more complicated.

Since a significant charging was found on the resist if the conductive layer was not introduced, it would be interesting to know how high the surface potential was generated on the resist surface. According to Miyazaki *et al.*[25], if we know the landing error, i.e. displacement value, the surface potential (V) can be obtained from the following equation:

$$D/B = -V/4U \quad (1)$$

where U is the electron-beam acceleration voltage, B is the distance of the target point from the centre of the chip on the sample at zero potential ($V=0$), and D is the registration error. From *Figure 10*, the registration error is around 5 μm. The chip size is 5 mm × 5 mm, so the last square to the centre of the chip is approximately 3.5 mm. Accelerating voltage for the electron-beam tool is 25 kV. By inserting all the numerical values into the above equation, a value of −143 V can be obtained for the surface potential. This value indicates that a significant large negative surface potential has been produced in the electron-beam exposure. If the surface potential of −1 V is assumed, the registration error will be 0.035 μm. Assuming for a moment that the space-charge density is uniform, the surface potential can be expressed as the equation below:

$$V = QT/2K \quad (2)$$

where Q is the amount of charge remaining in the insulator, K is the dielectric constant of the insulator and T is the thickness of the insulator. Since the relative dielectric constant for phenol-type resin is usually in the range of 5, we can assume the whole stack of insulator has a relative

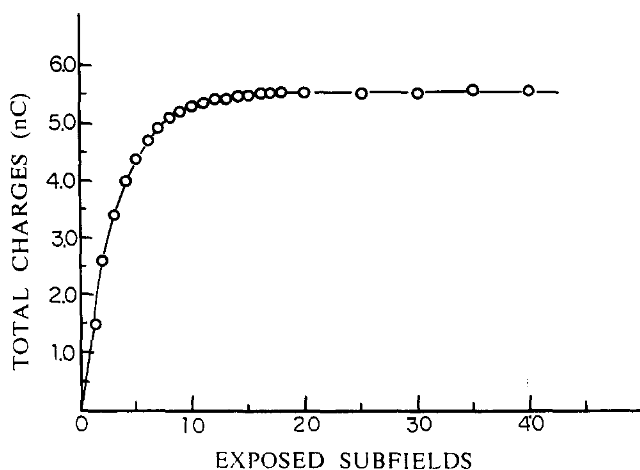

Figure 15 Total charge accumulated vs. the total number of subfields exposed. A calculated result using a simplified model

dielectric constant of 5. Therefore, the value for K is $5 \times 8.85 \times 10^{-14}\,\mathrm{A\,s\,V^{-1}\,cm^{-1}}$, the value for T is $4.2\,\mu$m, and V is 143 V calculated from equation (1). By inserting all these values into equation (2), $Q = 0.3\,\mu$C can be obtained. The total deposited charge on the wafer from the electron gun is $3.75\,\mu$C. This indicates that the amount of trapped charge is around 8%. Since we have the Q value, the capacitance of this configuration can be calculated by the equation below:

$$C = Q/V \tag{3}$$

The C value calculated from above is 2.1 nF. If we have the resistance of the discharge layer, we can calculate the RC time constant for charge dissipation assuming that the discharge process is a simple RC circuit. Since the conductivity of the discharge layer that we have been using in this study is around $10^{-1}\,\mathrm{S\,cm^{-1}}$, and the thickness for the top layer is around 1000 Å, the resistance R will be around $10^6\,\Omega$. A RC time constant of 2.1 ms can be obtained by simply multiplying R and C values. Here we assume that the capacitance will not change when the discharge layer is introduced. In the real situation, the capacitance may increase due to the charge spreading on the conductive layer.

For the electron-beam tool, an exposure cycle involves the exposure of each spot and then a step to the next spot, until the whole subfield is completed. After finishing one subfield, the beam steps to the next subfield. In this process, besides the exposure time there is a step time involved too. To simplify the system, we assume each subfield is a $100 \times 100\,\mu\mathrm{m}^2$ square, and the exposure of one subfield takes $665\,\mu$s. The charge will decay exponentially with time. When the beam moves from the first subfield to the next subfield, we assume the beam will be affected by 100% of the charge deposited on the first subfield. This is not true for two reasons: first, most of the electrons penetrate through the insulators; secondly, some charges have been diffused away during the exposure and step process in this $665\,\mu$s. Therefore, the result generated here will be an overestimate. We assume that when the beam moves to the third subfield, the first one will have $665\,\mu$s to dissipate the charge. With all these assumptions, we can obtain the relation between the total amount of charge remaining on the chip and the number of subfields that have been exposed. As shown in *Figure 15*, the additional charges added to the system are very insignificant after 15–20 subfields. It is also clearly shown that 90% of the charge is contributed by the last eight exposed subfields. The curve seems to level off near 5.5 nC. This amount of charge will only generate 2.6 V of surface potential on the resist. Our calculation was based on the assumption that all the charges deposited on the wafer were trapped on the insulator. If we assume only 8% of the deposited charges got trapped, the voltage will drop to 0.21 V. This magnitude of surface potential will not cause any significant landing error.

The charging effect of resists under electron-beam exposure seems to be affected by many factors, e.g. resist thickness, pattern density, electron-beam current, electron-beam exposure time, thickness of insulating layer underneath resist, type of resist, etc. We have already discussed some of the factors with a simplified model above. It is easy to understand the possible tendency when each factor is changed. However, to obtain accurate quantitative data is very difficult owing to the complexity of the system. Nevertheless, we have demonstrated that we can use poly(alkylthiophene) and water-soluble P3-ETS as discharge interlayer and top layer respectively to eliminate the charging problem in the electron-beam exposure. It is interesting that the conductivity ($10^{-1}\,\mathrm{S\,cm^{-1}}$) of processable polymer that we have obtained here in this study was not possible 10 years ago. Now, the electron-beam tools are moving from 25 kV to 50 and 100 kV, we may not need such highly conducting materials. On the other hand, the continued shrinkage of the circuitry dimension and increase in circuitry density will require higher precision in electron-beam direct write. It will be interesting to see if the application of this type of material in electron-beam lithography can become a common practice in the future just like the concept of using conducting polymer for plating through hole that we first introduced a few years ago[26–29].

ACKNOWLEDGEMENTS

The author would like to thank Marie Angelopoulos, Ranee Kwong, Rich Kaplan, Bob L. Dundatscheck and John G. Horvat for their invaluable discussions and technical support.

REFERENCES

1. Saitou, N., Munakata, C. and Maekawa, A. *Japan. J. Appl. Phys.* 1971, **10**, 351
2. Langner, G. O. 'Proc. Microcircuit Engineering '79', 1979, p. 261
3. Cummings, K. D. and Kiersh, M. *J. Vac. Sci. Technol.* (*B*) 1989, 7(6), 1536
4. Itoh, H., Nakamura, K. and Hayakawa, H. *J. Vac. Sci. Technol.* (*B*) 1989, 7(6), 1532
5. Yodokoro, Y. and Watanabe, H. *J. Vac. Sci. Technol.* (*B*) 1988, **6**, 357
6. Watanabe, H. and Todokoro, Y. *IEEE Trans. Electron Devices* 1989, **36**, 474
7. Tono-oka, Y., Sakanoto, K., Honda, T., Matsumoto, H. and Lida, Y. *SPIE* 1990, **1263**, 199
8. Kawasaki, Y., *et al.* Japan Patent 62113134
9. Angelopoulos, M., Shaw, J. M., Kaplan, R. D. and Perreault, S. *J. Vac. Sci. Technol.* (*B*) 1989, 7(6), 1519

10 Angelopoulos, M., Shaw, J. M., Lee, K.-L., Huang, W. S., Lecorre, M.-A. and Tissier, M. *J. Vac. Sci. Technol.* (*B*) 1991, **9**(6), 3428
11 Chiang, C. K., Druy, M. A., Gau, S. C., Heeger, A. J., Louis, E. J., MacDiarmid, A. G., Park, Y. W. and Shirakawa, H. *J. Am. Chem. Soc.* 1978, **100**, 1013
12 Tourillon, G. and Garnier, F. *J. Electrochem. Soc.* 1983, **130**, 2043
13 Jen, K. Y., Miller, G. G. and Elsenbaumer, R. L. *J. Chem. Soc., Chem. Commun.* 1986, 1346
14 Patil, A. O., Ikenoue, Y., Wudl, F. and Heeger, A. J. *J. Am. Chem. Soc.* 1987, **109**, 1858
15 Clark, T. C., Krounbi, M. T., Lee, V. Y. and Street, G. B. *J. Chem. Soc., Chem. Commun.* 1981, **8**, 384
16 Pitchumani, S. and Willig, F. *J. Chem. Soc., Chem. Commun.* 1979, **13**, 977
17 Angelopoulos, M., Shaw, J. M., Huang, W. S. and Kaplan, R. D. *Mol. Cryst. Liq. Cryst.* 1990, **189**, 221
18 Crivello, J. V. and Lam, J. H. W. *Macromolecules* 1977, **10**, 1307
19 Crivello, J. V. and Lam, J. H. W. *J. Polym. Sci., Polym. Chem. Edn.* 1979, **17**, 977
20 Saeva, F. D. and Morgan, B. P. *J. Am. Chem. Soc.* 1984, **106**, 421
21 Huang, W. S. and Park, J. M. Electrode Materials and Process for Energy Conversion and Storage, Electrochemical Society, Pennington, NJ, 1987, Vol. 87-12, p. 100
22 Huang, W. S., Angelopoulos, M. and Humphrey, B. D. 'Proc. SPE, ANTEC '91', 1991, p. 788
23 Ikenoue, Y., Saida, Y., Kira, M.-A., Tomozawa, H., Yashima, H. and Kobayashi, M. *J. Chem. Soc., Chem. Commun.* 1990, 1694
24 Patil, A. O., Ikenoue, Y., Basescu, N., Colaneri, N., Chen, J., Wudl, F. and Heeger, A. J. *Synth. Met.* 1987, **20**, 151
25 Miyazaki, M., Saitou, N. and Munakata, C. *J. Phys.* (*E*) 1981, **14**, 194
26 Huang, W. S., Angelopoulos, M., White, J. R. and Park, J. M. *Mol. Cryst. Liq. Cryst.* 1990, **189**, 227
27 Huang, W. S., Angelopoulos, M., Park, J. M. and White, J. R. 'Proc. SPE, ANTEC '91', 1991, p. 864
28 Gottesfeld, S., Uribe, F. A. and Armes, S. P. *J. Electrochem. Soc.* 1992, **139**, L14
29 Schering Subtraganth Compact CP product information sheet; Beator, K., Beussel, B. and Grapentin, H.-J. *Metalloberflache* 1992, **46**, 9